16th World Conference on Earthquake, 16WCEE 2017

Santiago Chile, January 9th to 13th 2017

Paper N° 3569

Registration Code: S-W1464738740

EFFECTS OF MOAT WALL IMPACT ON THE SEISMIC RESPONSE OF BASE ISOLATED NUCLEAR POWER PLANTS

A. Sarebanha [(1)], G. Mosqueda [(2)], M. K. Kim[(3)], J. H. Kim[(4)]

[(1)] *Graduate Research Assistant, University of California, San Diego, asareban@ucsd.edu*
[(2)] *Associate Professor, University of California, San Diego, gmosqueda@ucsd.edu*
[(3)] *Principal Researcher, Korea Atomic Energy Research Institute, minkyu@kaeri.re.kr*
[(4)] *Senior Researcher, Korea Atomic Energy Research Institute, jhankim@kaeri.re.kr*

Abstract

Seismic isolation can be an effective strategy to protect critical facilities including Nuclear Power Plants (NPPs) from the damaging effects of horizontal earthquake ground shaking. The increased flexibility at the base and resulting elongation of the natural vibration period of the structure leads to significant reductions in acceleration and forces transmitted to the structure above the isolation level at the expense of large displacements in the isolation system. To accommodate these displacements, the isolated structure requires a large horizontal clearance or moat at the basement level. The surrounding moat wall around the clearance is intended to function as a hard stop to limit isolation system displacements. In the case of an extreme earthquake, there exists the potential for impact of the isolated structure to the moat wall. This impact is of significant concern especially in NPPs due to the potential for increased transfer of forces and amplification in response of the structural system, piping and other contents. However, the consequences of impact or factors important to mitigate its effects are not very well understood. To address this concern, this study examines simple NPP models to capture the impact forces and the effects of impact on the response of seismically isolated NPPs. Characteristics of the isolation hardware and hard stop that minimize the effects of impact are also examined by considering variable distances to the hard stop and properties of the moat wall and isolation system. The amplification in response is reported for acceleration and floor spectral accelerations at different points along the height of a simplified model of a containment structure. Results of these studies indicate the moat wall can have significant penetration, and thus not fully limit displacement, while having significant increases in accelerations throughout the height of the NPP model.

Keywords: nuclear power plant; seismic isolation; moat wall impact

1. Introduction

Seismic isolation can be an effective strategy to protect critical facilities including Nuclear Power Plants (NPPs) from the damaging effects of horizontal seismic loads. Application of seismic isolation in NPPs can lead to a simplification of seismic designs, enhanced safety margin, and facilitate standardization [1]. Seismic isolation is typically achieved by installing a layer of flexible bearings at the base of the structure. The increased flexibility and resulting elongation of the natural vibration period of the structure leads to significant reductions in acceleration and forces transmitted to the structure above the isolation level at the expense of large displacements in the isolation system hardware. To accommodate these displacements, the isolated structure requires a horizontal clearance or a moat at the basement level. The allowable displacement is often limited by a moat wall that is also intended to function as a hard stop and prevent failure of the bearings that support the NPP [2].

The majority of past experimental and numerical research on seismic isolation has mainly focused on verifying the effectiveness of the technology for design level response. While extreme earthquakes are also of concern for non-isolated structures, the potential impact to a hard stop in NPPs requires a thorough examination due to the increased transfer of forces and amplification in response of the structural system, piping and other contents. Importantly, the consequences of impact or factors to mitigate these effects have not been investigated. In this study, the effects of impact on the response of seismically isolated NPPs are examined and characteristics of the isolation hardware and hard stop that minimize these effects identified. The development of a simplified model that can capture the impact forces is also described.

2. Simplified Model of Nuclear Power Plant

A key focus of this study is on the effects of moat wall impact on seismic response of base isolated NPPs, including the development of a model to capture this behavior. A range of parameters were considered for the isolation devices, the moat wall, and distance to the moat wall. To this end, a simplified lumped-mass stick model of a NPP based on the APR1400 plant model [3] was considered. The properties of the simplified model were calculated to give similar dynamic properties, particularly for the containment structure. The mass of the structure and the secondary systems was lumped at discrete locations at select levels. As recommended by Giammona et al. [4], damping was assumed to be zero for isolation modes of vibration and 5% for all the other superstructure modes. The structural model was programmed in OpenSees [5] to make it more conducive to conduct numerous parametric studies and take advantage of the larger element library for modeling complex and nonlinear behavior of the structure including impact.

3. Moat Wall Model

Guidelines for the seismic design of isolated NPPs will prescribe a hard stop or displacement restraint at no less than 90th percentile BDBE (Beyond Design Basis Earthquake) displacement along each axis [2]. Consequently, the probability of impact is sufficiently small that it is typically not considered in design. However, it is important to examine the consequences of such an impact should it occur. The hard stop is likely be constructed in the form of a moat wall around the basement of the NPP. In this study aimed at studying the effects of seismic pounding in NPPs, different Clearance to Hard Stop (CHS) values were assumed to examine the effect of this parameter. Modeling of the moat wall as the hard stop required consideration of the concrete wall and soil backfill in the structural model as well as localized impact behavior [6]. While several previous studies have examined impact behavior for buildings both experimentally [7] and numerically [8, 9], the impact behavior is expected to have different characteristics due to size and thickness of the basemat and moat walls in the case of isolated NPPs. Figure 1 below shows a schematic of the isolation level of the NPP and the surrounding moat wall. Unlike previous studies that have examined impact in isolated buildings, it is expected that the wall to basemat contact surface and the thickness of these components can be one order of magnitude larger and thus requires revisiting the moat wall impact models.

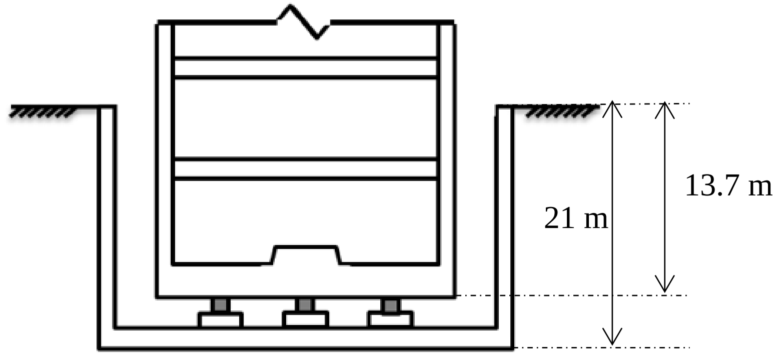

Fig. 1 – Schematic view of NPP with moat wall and backfill soil

In past decades, studies of pounding in base isolated structures has been mainly analytical with various approaches used to model this phenomena. Information on modeling the behavior of the moat wall with soil backfill under impact forces as required here is limited in the literature, particularly for the case for NPP with the contact areas consisting of massive plane surfaces. To address this need and better estimate the properties of the moat wall under impact forces, FEM analysis were performed using LS-Dyna. Impact between the slab and the moat wall was studied in detail by modeling a unit width (1 ft. or 0.3048 m) of the slab and moat wall. The calibrated density of the slab material was provided to represent the mass per unit length of the NPP structure. An assumed initial velocity was assigned to the slab to simulate the impact. Based on the observed behavior, a new macro model was developed for the moat wall considering impact in the NPP structure.

In the FEM analysis, the moat wall was modeled as a reinforced concrete wall with solid elements for concrete and beam elements for reinforcement bars with MAT_WINFRITH_CONCRTE (084/085) and MAT_PLASTIC_KINEMATIC (003) material models used to model concrete and steel respectively in the analysis. To constrain the reinforcement bars into the concrete, the Lagrange in Solid constraint was used. It should be noted that in cases where the concrete undergoes severe damage, this method may not be accurate. Modeling details for the moat wall such as dimensions, material properties, and reinforcements are described in detail in the next section. The contact algorithm (*CONTACT_AUTOMATIC_SURFACE_TO_SURFACE) in LS-Dyna was used to model the contact between the slab and the moat wall. This algorithm uses a penalty method with the scale factor on the default slave penalty stiffness set to 5 in order to avoid element penetrations of the slab into the moat wall with both having the same material properties. In LS-Dyna, the initial integration time-step can be defined manually while the required time-step to ensure convergence is calculated automatically before starting the analysis. In cases with contact, the analysis time-step could be very small.

The LS-DYNA simulation results were used to develop a macro model of the moat wall considering impact. The model consists of a representative hertz damped spring mode for the impact interface, modeling the moat wall dynamic force-displacement behavior, and spring to capture the soil backfill contributions. These analyses showed the deformation of the moat wall at this scale due to impact does not follow the previous assumption of a cantilever column with a point load simulating the contact with the base floor slab [8]. Therefore, a new model was proposed to be able to better capture the behavior of the moat wall with a larger impact surface as observed in the FEM simulations (Figure 2). This model consists a rigid section for the moat wall along the height where impact is expected with the slab and an elastic beam element for the lower section connecting to the base. These elements were connected using non-linear rotational spring to represent the moment rotation behavior of the assumed section. The nonlinear rotational springs were placed at the locations of the largest observed curvature during the FEM analysis.

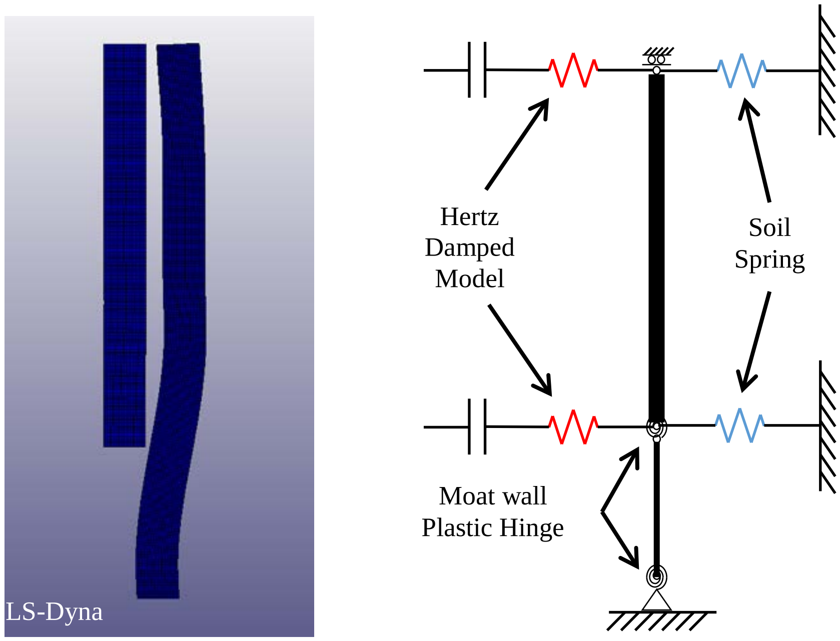

Fig. 2 – Slab and moat wall deformed shape modeled in LS-Dyna (left), new macro model (right)

3.1 Moat wall

For this study, the moat wall model was assumed to be approximately 20 m high, 1.5 m thick, and 49 m wide based on a preliminary design. Confined concrete was considered to model the core material in the moat wall section($f_c' = 34\ MPa$) with grade 60 steel considered for the reinforcement. The longitudinal reinforcement ratio (ρ_s) was assumed to be 0.06 % with shear reinforcement considered. Moment-rotation behavior for the assumed section was first examined using SAP2000 with the results shown in Figure 3. These results were used to obtain parameters for the nonlinear rotational spring models used in OpenSees model capture the moat wall plastic hinge regions.

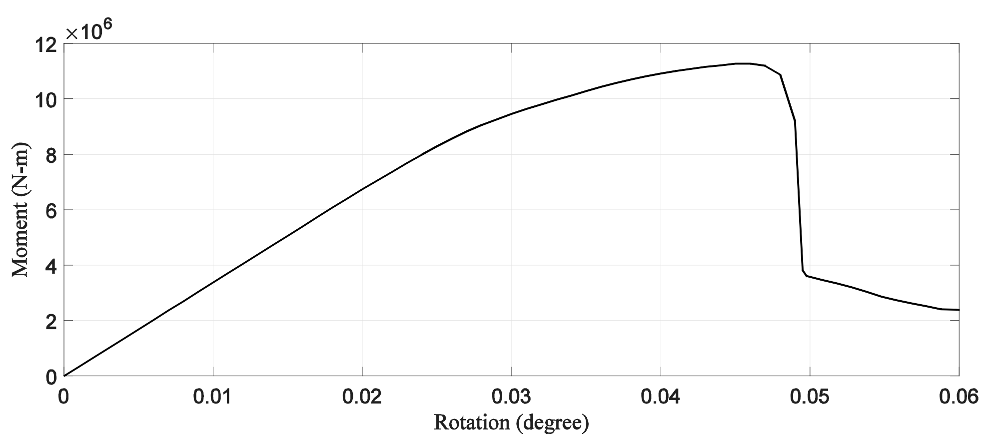

Fig. 3 – Moment rotation behavior using SAP2000 for 0.3048 m (1 ft.) width of the wall

3.2 Soil Model

The backfill soil was assumed to be coarse gravel to represent stiff behavior and modeled using the nonlinear Hyperbolic Force Displacement (HFD) hyperbolic model [10]. Soil properties and parameters for model are listed in Table 1. This model was originally developed for soil-abutment-bridge structure interaction and reported parameters were originally derived for a 1.67 m high retaining wall. Soil stiffness and maximum abutment force are dependent on the height of the moat wall. Therefore, extrapolation was considered to calculate the properties at 20 m depth.

Table 1 – Soil Properties and parameters for HFD model

Mass Density	23565 N/m.^{3}	HFD model parameters	
Poisson's ratio	0.33	Ultimate force F_{ult}	2017 kN
Angle of friction , φ	40°	y_{max}	4.0 cm
Modulus of elasticity	76,129 kN/m^2	Kmax (per m of soil)	264 kN/cm

The soil was modeled in OpenSees using HFD model with HyperbolicGapMaterial. This element requires knowledge of ultimate passive resistance, initial stiffness and unloading/reloading stiffness of the soil. The assumed parameters for this model are listed in Table 2.

Table 2 – HyperbolicGapMaterial properties in used in OpenSees

Top soil spring (tributary length 7.5m)	Ultimate force (F_{ult} [kN])	1449342.68
	Initial stiffness (K_{max} [$\frac{kN}{m}$])	5033586.67
Middle soil spring (tributary length 12.5m)	Ultimate force (F_{ult} [kN])	2415569.46
	Initial stiffness (K_{max} [$\frac{kN}{m}$])	8389309.43
Unloading/reloading stiffness (K_{ur})		$10 \times K_{max}$
Failure ratio (R_f)		1.0

3.3 Impact Model

One of the most challenging aspects of the proposed simulations was modeling of the impact interface. The Hertz model was originally proposed for static contact of two bodies, in which stresses and deformations near the contact point are described as a function of the geometric and elastic properties of the bodies [6]. The contact force is related to the relative indentation of two bodies with a nonlinear spring. This stiffness, K_h depends on material properties and shape of impacting bodies and can be calculated as

$$K_h = \frac{4}{3\pi}\left(\frac{1}{\lambda_1+\lambda_2}\right)\sqrt{\frac{R_1 R_2}{R_1+R_2}} \tag{1}$$

$$K_h = \frac{4}{3\pi}\left(\frac{1}{\lambda_1+\lambda_2}\right)\sqrt{R_1} \tag{2}$$

$$\lambda_h = \frac{1-\nu_i^2}{\pi E_i} \tag{3}$$

for two colliding spheres with radius of R_1 and R_2,and colliding spheres of radius R_1 to a massive plane surface while λ_i is a material properties and is related to E_i (Modulus of Elasticity) and ν_i (Poisson's Ratio). In case that colliding bodies are not spheres, an equivalent spheres radii could be used to calculate the impact stiffnesses.

The original Hertz contact law appears to predict the impact force, however, this model does not capture the energy dissipation due to impact. An improved version of the modeled was introduced with a nonlinear damper in conjunction with the Hertz Spring [11](Figure 4). In this model, the contact force is given by:

$$F_c = K_h \delta^{3/2} + \xi \delta^{3/2} \dot{\delta} \tag{4}$$

where $\dot{\delta}$ is penetration velocity and ξ is the damping coefficient and prescribed as a function of the coefficient of restitution (e), hertz stiffness, and penetration velocity as follows:

$$\xi = \frac{8}{5}\frac{K_h(1-e)}{e\dot{\delta}} \quad (5)$$

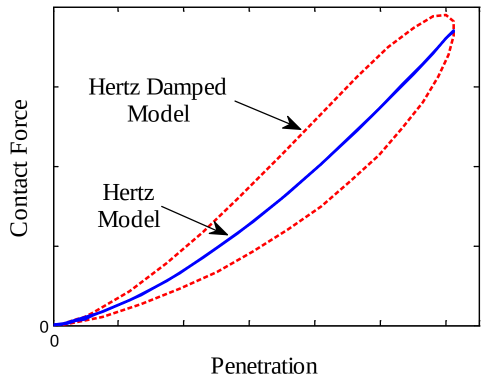

Fig. 4 – Contact Force-Penetration relation for Hertz and Hertz Damped Model [8]

This hertz damped model was modeled in OpenSees using the available Impact Material. The required parameters for this material model are:

- Gap: corresponds to clearance to hard stop (discussed later)
- Equivalent spring stiffness using Eq. 2 where R_1 is assumed radius of the equivalent sphere volume of the moat wall
- Coefficient of restitution (e) : 0.8
- Ratio of yield displacement over maximum displacement (a) : 0.1

3.4 Implementation of Impact, Moat wall and Backfill Soil

Figure 5 shows the implementation of the impact, moat wall and backfill soil models on the sides of the simplified NPP 2D model. The response will be compared later at Node 707 identified on the figure.

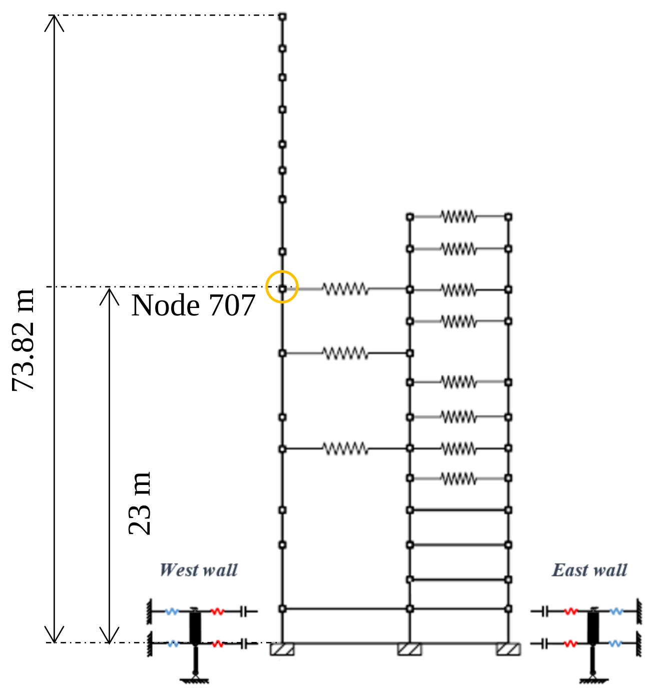

Fig. 5 – NPP with Moat wall Model

4. Parametric Study

In order to study the effect of different properties for the impact in the NPP, different cases had been considered for ground motions, intensity levels, Clearance to Hard Stops (CHS), material properties, and different stiffness ratios for the isolators.

4.1 Ground Motions (GM):

Records for three different earthquakes were considered to use for this study as listed in Table 3. These records were obtained from NGA database [12]. Two horizontal components of these records were used in the simulation.

Table 3 – Ground Motion (GM) used in simulations

GM	1	Chi-Chi	NGA_no_1508_TCU072-E	60.0 sec.
	2		NGA_no_1508_TCU072-N	60.3 sec.
	3	Imperial Valley	NGA_no_180_H-E05140	34.0 sec
	4		NGA_no_180_H-E05230	37.0 sec.
	5	Loma Prieta	NGA_no_779_LGP000	23.6 sec.
	6		NGA_no_779_LGP090	22.5 sec.

4.2 Intensity Level (IL):

Ground motions were scaled to fit the RG1.60 Revision 2 design response spectrum [13] for DBE motion scaled to 0.5g without distortion. In order to examine the Beyond Design Basis Earthquake (BDBE), ground motion were scaled by a factor of 2 (which is more conservative than the recommended values of 150 % per ASCE 4 [14]). Moreover, to be able to further study the effect of impact, another case was considered which corresponds to spectral acceleration of 1.25 g since impact is more likely to occur at this intensity for most ground motions. Figure 6 shows spectral acceleration for different ground motions used for nonlinear response history analysis.

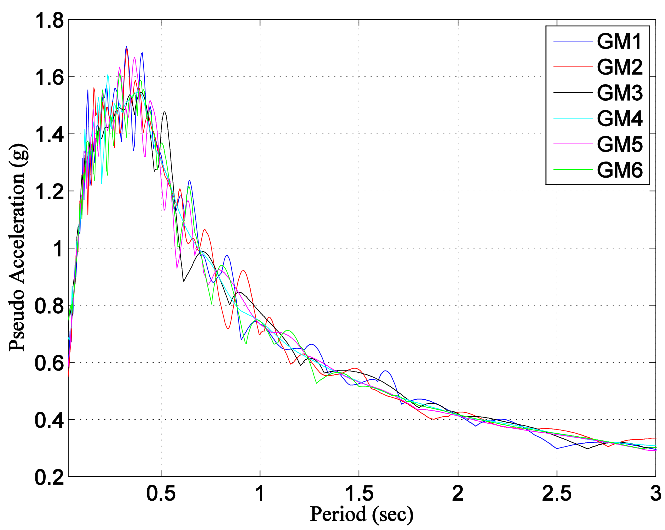

Fig. 6 – Spectra acceleration (5% damping) for different GMs – scaled for 0.5 g

4.3 Clearance to Hard Stop (CHS):

Three different cases were considered for the CHS. Based on prototype bearings designed for seismic isolation of the APR1400 with design displacement (D_d) of 0.21m (design shear strain of 100%), values were selected based on 350, 400, and 450 % of the design displacement. Typically, lead rubber bearings are designed and experimentally tested for shear strain well below this level, experimental testing have shown full scale bearings to reach 450% shear strain prior to failure. The nonlinear behavior of the bearing under extreme loadings requires further investigation in order to develop models that capture their behavior at this level of loading [15].

Table 4 – Different case considered for Clearance to Hard Stop (CHS)

CHS/D_d	350%	400%	450%
CHS (m)	0.735	0.84	0.945

4.4 Material Properties:

In order to account for variation in properties of the isolators, three different cases were considered: Lower Bound (LB), Nominal Values (NV), and Upper Bound (UB). Measured properties of the isolators from prototype testing were considered to be the Nominal Values. The LB and UB properties were calculated using conservative property modification factors based on AASHTO [16] and MCEER [17] (Table 5).

Table 5 – Calculated bounded properties using property modification factors

	NV	Bound values		Total Modification	Different Property Modification			
					Aging	Scragging	Temperature	Material
K_1 (kN/m)	1870128.02	1870128.02	LB	1	1	1	1	1
		2262855.84	UB	1.21	1.1	1	1.1	1
f_y (kN)	46954.24	32867.96	LB	0.7	1	1	1	0.7
		61979.59	UB	1.32	1.1	1	1.2	1

4.5 Bearing model parameters

The bearings were modeled as having bi-linear coupled behavior represented by a Bouc-wen model [18]with the secant slope stiffness selected to give an isolated period of the superstructure of 2.0 sec. Two different cases were considered for the initial stiffness as prescribed as a ratio of the second slope stiffness (K_2): 0.1 to represent lead rubber isolators and 0.01 to represent friction type isolators.

4.6 Different Case Studies

For each Intensity Levels (0.5, 1.0, and 1.25 g), and different isolator material properties (LB, NV, and UB), 36 different cases were considered and simulated using the models developed in OpenSees. Table 6 shows the information for each case considered.

Table 6 – Cases considered in parametric study

Case #	GM	CHS	K2/K1	Case #	GM	CHS	K2/K1	Case #	GM	CHS	K2/K1
1	1	350%	0.1	13	3	350%	0.1	25	5	350%	0.1
2			0.01	14			0.01	26			0.01
3		400%	0.1	15		400%	0.1	27		400%	0.1
4			0.01	16			0.01	28			0.01
5		450%	0.1	17		450%	0.1	29		450%	0.1
6			0.01	18			0.01	30			0.01
7	2	350%	0.1	19	4	350%	0.1	31	6	350%	0.1
8			0.01	20			0.01	32			0.01
9		400%	0.1	21		400%	0.1	33		400%	0.1
10			0.01	22			0.01	34			0.01
11		450%	0.1	23		450%	0.1	35		450%	0.1
12			0.01	24			0.01	36			0.01

5. Results

A total of 324 different simulations were conducted with variations of the different parameters described in Table 6. For the seismic intensity level 0.5 g, no impact occurred between the NPP and the moat wall. However, impacts were observed for the higher intensity levels. As expected, using the bearing LB properties resulted in more cases with impact. For intensity level equals to 1.0 g, 58.3 %, 33.3%, and 5.5 % cases with impact were observed for LB, NV and UB bearing properties respectively. The ratio of impact cases are 100, 80.6, and 50 % for 1.25 g intensity level (Figure 7).

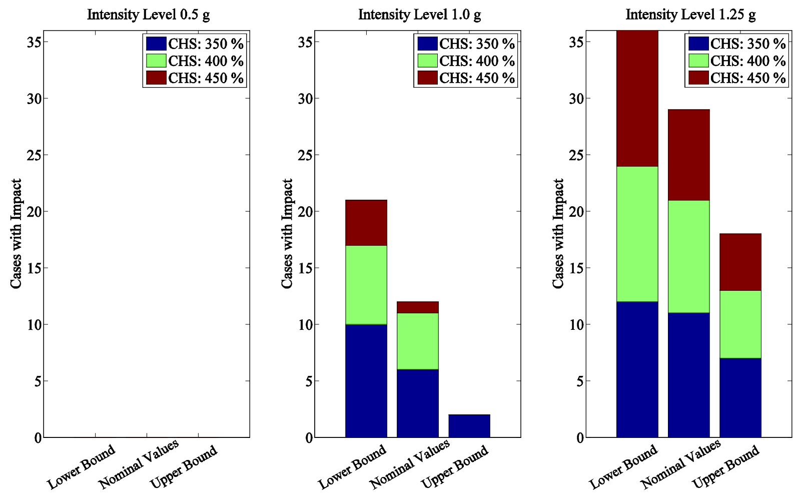

Fig. 7 – Impact cases for different GM Intensity Levels

For all cases considered in this parametric analysis, displacement demands normalized by CHS are presented in Figure 8. Also, the same simulations were run without the moat wall to evaluate the displacement demand. These plots indicate by how much the displacement demands exceed the CHS and how the moat wall reduces these displacement demands. Cases with a ratio less than one indicates that the seismic isolation displacement demand was less than the provided clearance and did not impact. As Figure 8 shows, for cases where impact did occur, the presence of the moat wall and backfill soil reduced the displacement demand on the bearings although there was still significant penetration into the hard stop. Also, in some cases implementation of hardstop resulted in increased displacement demand for the isolator compared with the case for no hardstop simulations (i.e. IL=1.25 – case 31). This increase is mainly due to the rebound effect of the NPP structure after the first impact in the one direction, which led to higher displacement demand in the other direction.

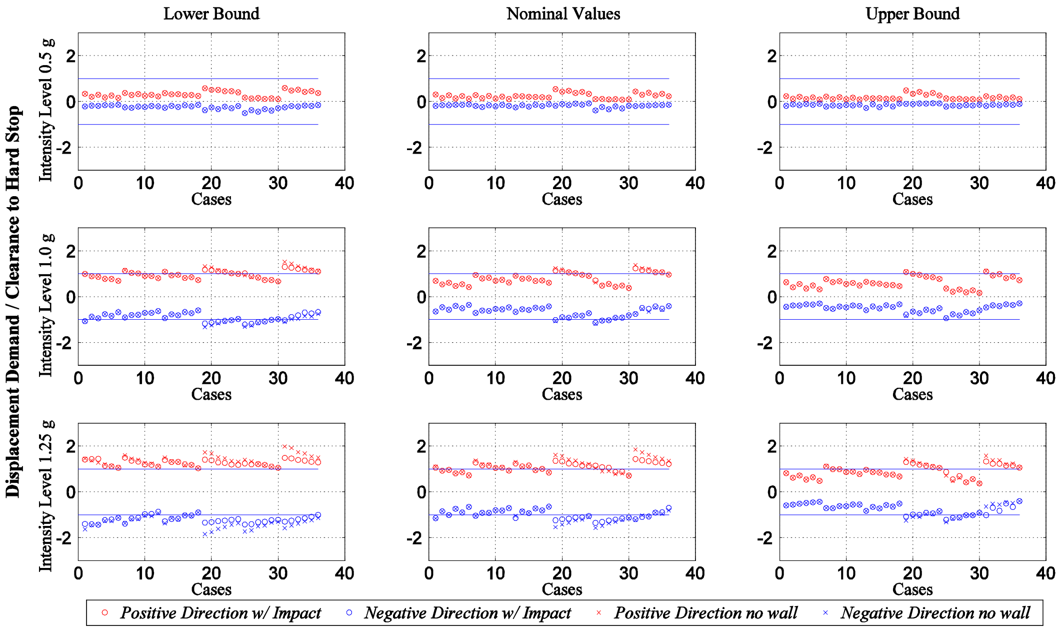

Fig. 8 – Displacement demand normalized by clearance to hard stop

Seismic pounding to the moat wall increased the superstructure response including accelerations, which may lead to damage of non-structural components. For this analysis, absolute acceleration at node 707 identified in Figure 5 is examined. Figures 9-10 show the peak absolute acceleration for all cases with and without moat wall (impact model) for positive and negative directions. Although not identified here, the acceleration increase in one direction corresponds to the first impact while the second impact on the opposite side, which is typical, increases acceleration in the other direction. This increase in absolute acceleration can be up to 2.24 and 2.37 times in positive and negative directions for intensity level of 1.0 g corresponding to BDBE events.

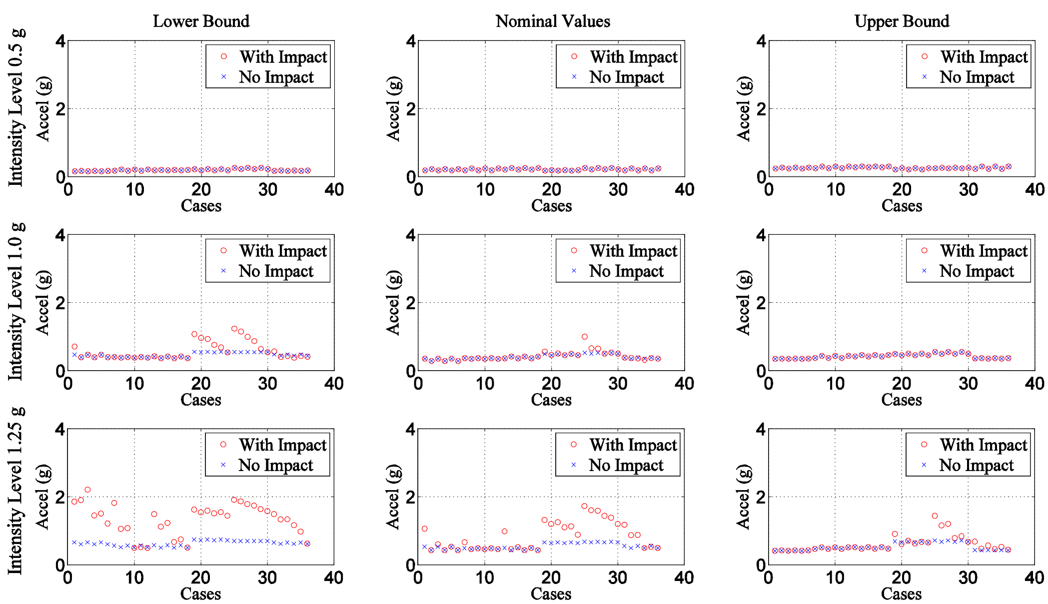

Fig. 9 – Positive acceleration at elevation 23m

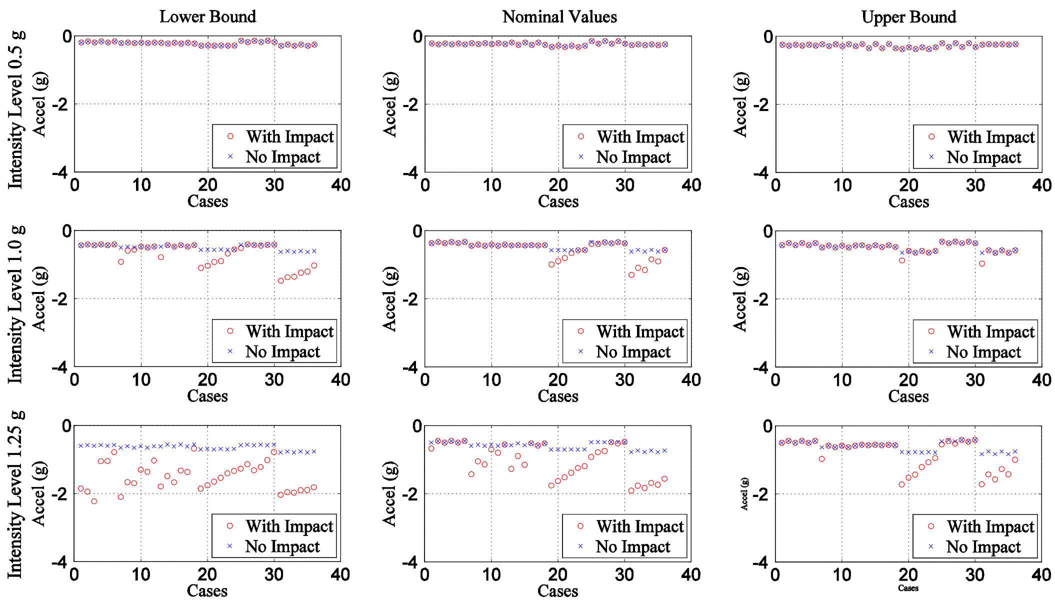

Fig. 10 – Negative acceleration at elevation 23 m

To gain a better insight into the actual response of NPP with impact, more detailed analysis results are presented for case 25 with NV properties for IL of 1.0 g. The displacement demand of the isolation systems is shown in Figure 11a while the acceleration response for a selected node 707 is shown in Figure 11b. It is evident from these figures that the reduction in displacements is small while the increase in acceleration is a factor of two. Isolator hysteresis loop are presented in Figure 11c. Floor response spectra for node 707 clearly shows an increase (up to 3 times) in the demand which may result in increased non-structural damage in the structure (Figure 11d). Impact force deformation for hertz impact element shows that impact only occurred in the negative direction (Figure 11e). Force deformation of the modeled backfill soil is also presented in Figure 11f.

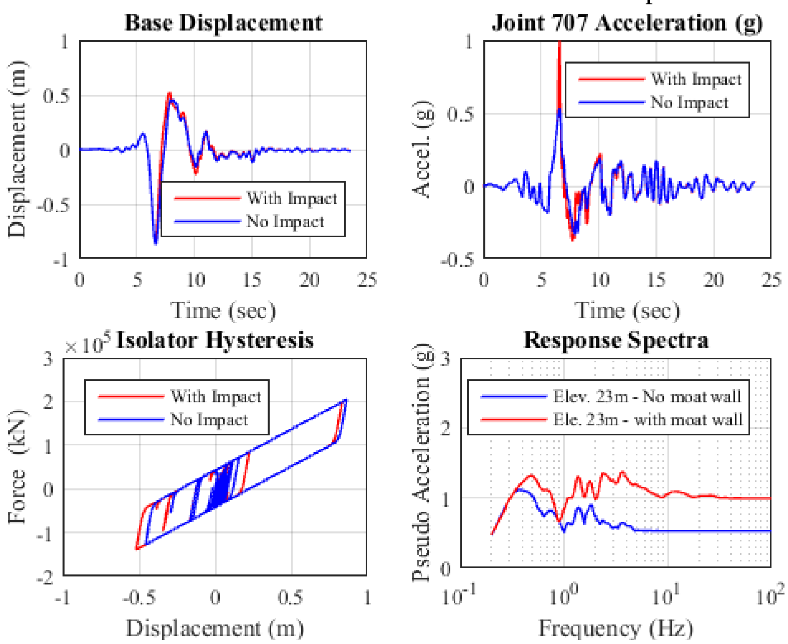

(a) (b)

(c) (d)

(e)

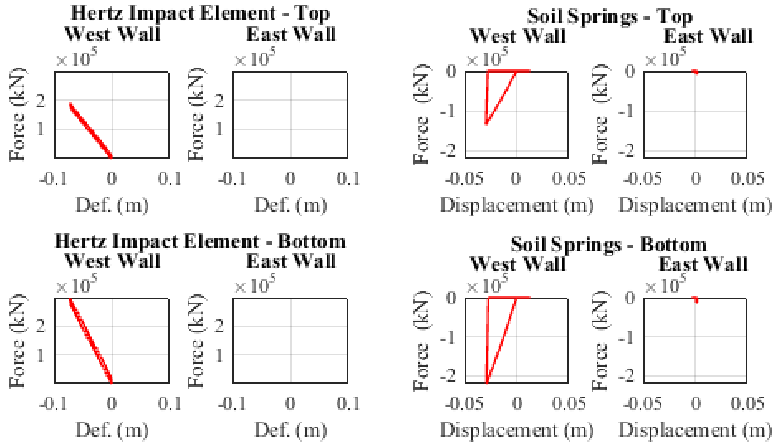

(f)

Fig. 11 – GM 5: Loma Prieta, CHS: 350 % (0.735 m), IL: 1.0 g , NV, K2/K1 ratio = 0.1 (Case 25) (a) base displacement time history, (b) acceleration at elevation 23 m, (c) isolator hysteresis loop, (d) floor response acceleration at ele. 23 m (e) hertz impact force, (f) backfill soil force deformation

6. Summary and Conclusion

The main contributions of this paper are related to modeling of seismically isolated NPP with moat wall impact and insight into the effects of impact on the superstructure response. A macro model to capture the impact forces was developed in OpenSees based on observed behavior of a finite element model in LS-Dyna. Results from parametric studies of the performance of the NPP under different seismic intensity levels and various properties for the bearings and moat wall including clearance to hard stop was presented. Based on these results, variation in the isolator properties should be considered when examining seismic pounding. For the ground motions considered here at BDBE, 58.5 % cases resulted in impact for lower bound properties while only 5.5 % of cases for upper bound properties. Since the impact results are dependent on the assumed bearing properties, variations in behavior can be obtained from the experimental testing under large shear strains. Implementation of a moat wall as a hard stop for isolated NPP is able to decrease the displacement demand. However, since the NPP is relatively heavy structure designed to remain elastic during a seismic event, consideration of the moat wall and backfill soil flexibility resulted in significant penetration into the wall. As a result, isolators can undergo displacements larger than their design limit based on the clearance to hard stop, indicating the need to test the bearings beyond the hard stop to ensure functionality in the case of an extreme earthquake. Variability in the properties of the moat wall also needs to be examined. As a result of impact, the absolute accelerations was found to increase by factors up to 2.4 along the height of the NPP compared to a similar simulation without a moat wall.

7. Acknowledgments

This research was supported by the Korea Atomic Energy Research Institute (KAERI). Any opinions, findings, conclusions, and recommendations presented herein are those of the authors and do not necessarily reflect the views of the sponsor.

8. References

[1] Tajirian, F. F., Kelly, J. M., and Aiken, I. D. (1990): Seismic Isolation of Advanced Nuclear Power Sations. *Earthquake Spectra*, **6** (2), 371-401.

[2] Kumar, M., and Whittaker, A. S. (2015): On the Calculation of the Clearance to the Hard Stop for Seismically Isolated Nuclear Power Plants. *SMiRT-23*, Manchester, United Kingdom.

[3] Kim, H.-G. (2005): The Design Characteristics of the Advanced Power Reactor 1400. *ICONE-13*, Beijing, China.

[4] Giammona, A. P., Ryan, K. L., and Dao, N. D. (2014): Evaluation of Assumptions Used in Engineering Practice to Model Buildings Isolated with Triple Pendulum(TM) Isolators in SAP2000. *Earthquake Spectra*, **31** (2), 637-660.

[5] OpenSees (2014): Open system for earthquake engineering simulation (Version 2.4.4) [computer software]. <available online at: http://opensees.berkeley.edu/>.

[6] Goldsmith, W. (2001): *Impact: The Theory and Physical Behvaior of Colliding Solids*. Dover Publication, New York.

[7] Masroor, A., and Mosqueda, G. (2012): Experimental simulation of base-isolated buildings pounding against moat wall and effects on superstructure response. *Earthquake Engineering & Structural Dynamics*, **41** (14), 2093-2109.

[8] Masroor, A., and Mosqueda, G. (2013): Impact model for simulation of base isolated buildings impacting flexible moat walls. *Earthquake Engineering & Structural Dynamics*, **42** (3), 357-376.

[9] Komodromos, P., Polycarpou, P. C., Papaloizou, L., and Phocas, M. C. (2007): Response of seismically isolated buildings considering poundings. *Earthquake Engineering & Structural Dynamics*, **36** (12), 1605-1622.

[10] Shamsabadi, A., Rollins, K., and Kapuskar, M. (2007): Nonlinear Soil–Abutment–Bridge Structure Interaction for Seismic Performance-Based Design. *Journal of Geotechnical and Geoenvironmental Engineering*, **133** (6), 707-720.

[11] Muthukumar, S., and DesRoches, R. (2006): A Hertz contact model with non-linear damping for pounding simulation. *Earthquake Engineering & Structural Dynamics*, **35** (7), 811-828.

[12] Ancheta, T. D., Darragh, R. B., Stewart, J. P., Seyhan, E., Silva, W. J., Chiou, B. S. J., Wooddell, K. E., Graves, R. W., Kottke, A. R., Boore, D. M., Kishida, T., and Donahue, J. L. (May 2013): PEER NGA-West2 Database. Pacific Earthquake Engineering Research Center, University of California, Berkeley, Berkeley, CA.

[13] United States Nuclear Regulatory Commission (USNRC). (2014): Regulatory Guide 1.60 Design Response Spectra for Seismic Design of Nuclear Power Plants. NUREG, Washington, DC.

[14] American Society of Civil Engineers (ASCE). (forthcoming): Seismic analysis of safety-related nuclear structures. ASCE 4-**, Reston, VA.

[15] Schellenberg, A. H., Sarebanha, A., Schoettler, M. J., Mosqueda, G., Benzoni, G., and Mahin, S. A. (2015): Hybrid Simulation of Seismic Isolation Systems Applied to an APR-1400 Nuclear Power Plant. *Technical Report PEER 2015/05,* Pacific Earthquake Engineering Research Center, University of California, Berkeley, Berkeley, CA.

[16] AASHTO (1999): Guide Specifications for Seismic Isolation Design. American Association of State Highwayand Transportation Officials, Washington, D.C.

[17] M.C. Constantinou, A.S. Whittaker, Y. Kalpakidis, D.M. Fenz , and Warn, G. P. (2007): Performance of Seismic Isolation Hardware under Service and Seismic Loading. MCEER-07-0012, Multidisciplinary Center for Earthquake Engineering Research, State University of New York at Buffalo, Buffalo, NY.

[18] Casciati, F. (1989): Stochastic Dynamics of Hysteretic Media. *Structural safety*, **6**, 259-269.